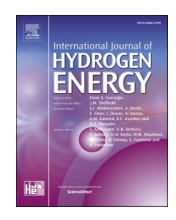
ELSEVIER

Contents lists available at ScienceDirect

International Journal of Hydrogen Energy

journal homepage: www.elsevier.com/locate/he





An atomistic study on the HELP mechanism of hydrogen embrittlement in pure metal Fe

Md Shahrier Hasan ^{a,**}, Mehmet Fazil Kapci ^b, Burak Bal ^b, Motomichi Koyama ^c, Hadia Bayat ^a, Wenwu Xu ^{a,*}

- ^a Department of Mechanical Engineering, San Diego State University, San Diego, CA, 92182, United States
- ^b Department of Mechanical Engineering, Abdullah Gul University, Sumer Campus, 38080, Kayseri, Turkey
- ^c Institute for Materials Research, Tohoku University, 2-1-1 Katahira, Aoba-ku, Sendai, 980-8577, Japan

ARTICLE INFO

Keywords:
Hydrogen embrittlement
HELP mechanism
Atomistic modeling
Iron
Hydrogen

ABSTRACT

The Hydrogen Enhanced Localized Plasticity (HELP) mechanism is one of the most important theories explaining Hydrogen Embrittlement in metallic materials. While much research has focused on hydrogen's impact on dislocation core structure and dislocation mobility, its effect on local dislocation density and plasticity remains less explored. This study examines both aspects using two distinct atomistic simulations: one for a single edge dislocation under shear and another for a bulk model under cyclic loading, both across varying hydrogen concentrations. We find that hydrogen stabilizes the edge dislocation and exhibits a dual impact on dislocation mobility. Specifically, mobility increases below a shear load of 900 MPa but progressively decreases above this threshold. Furthermore, dislocation accumulation is notably suppressed at around 1 % hydrogen concentration. These findings offer key insights for future research on Hydrogen Embrittlement, particularly in fatigue scenarios.

1. Introduction

Hydrogen (H) based energy technologies hold promise for the future, from fusion reactors to H cells. H is touted as a critical element for energy generation and energy storage due to its abundance, easy sourcing and zero carbon footprint. However, the increased use of H presents a challenge - the H embrittlement of metals and alloys. This phenomenon occurs when H atoms infiltrate metals, compromising their mechanical properties. As metals and alloys are foundational for structural applications [1–3], H embrittlement poses challenges for the future engineering and manufacturing [4–8].

Despite extensive research, the mechanism behind the detrimental effect of H on metals remains debated. A prevalent theory, the H-enhanced decohesion (HEDE), posits that H facilitates crack formation and growth in polycrystalline metals by promoting decohesion at crack tips [9]. Another explanation of H embrittlement suggests that H accelerates formation of vacancies, weakening the metal [10,11]. It is worth noting that while HEDE is theoretically robust, experimental evidence is inconclusive. The above mechanisms explain brittle fractures,

they do not account for ductile fractures - the primary failure mode in metals and alloys. Ductile failure begins with the micro-void formation near the second phase particle or precipitate in metals and alloys, followed by void coalescence and growth culminating in ductile failure. The H-enhanced Localized Plasticity (HELP) mechanism proposes that H assists local plastic deformation in metals [12–14]. According to HELP mechanism, presence of H eases dislocation motion, reduces dislocation-dislocation interaction known as H shielding and promotes dislocation nucleation locally softening the material. This theory gains support from observation showing reduced dislocation pile-up distances in metals like steels and aluminum with higher H concentration.

Attempts have been made to understand HELP mechanism through modeling at multiple scales [15–19]. At the electronic scale, Density Functional Theory (DFT) revealed that H increases Density of States (DOS) of the electron adjacent to the Fermi level resulting in enhanced local concentration of the free electron and decrease in elastic modulus [20,21]. Tehranchi et al. conducted an atomistic study where possible mechanisms of H induced softening was investigated [22]. For pure FCC Ni, no softening mechanism was found in the atomistic study, but it was

E-mail addresses: mhasan3719@sdsu.edu (M.S. Hasan), wenwu.xu@sdsu.edu (W. Xu).

https://doi.org/10.1016/j.ijhydene.2023.12.274

^{*} Corresponding author.

^{**} Corresponding author.

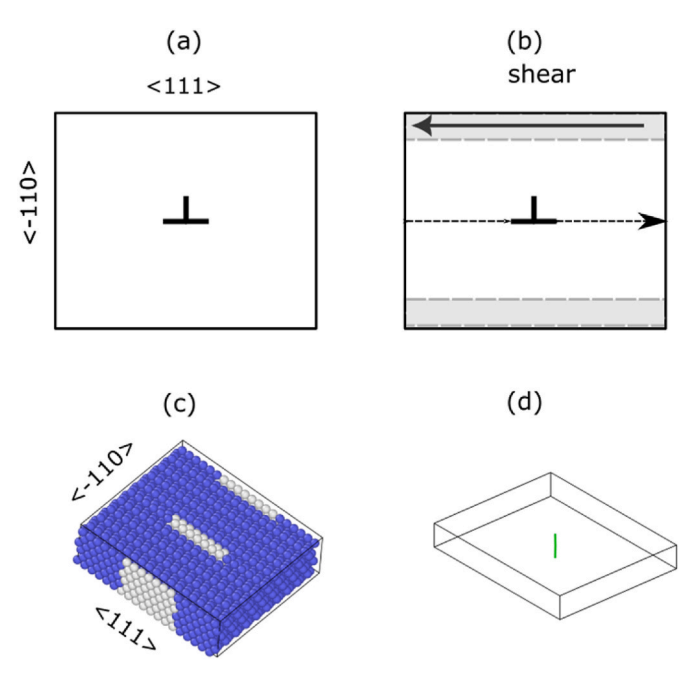


Fig. 1. Schematic diagram and Atomistic PAD model of pure metal Fe. (a) and (b) show schematic diagram of dislocation in PAD model at rest and under shear, respectively. (c) shows the atomistic PAD model where blue and white atoms represent matrix and dislocation core atoms respectively. (d) shows line representation of the edge dislocation. (For interpretation of the references to colour in this figure legend, the reader is referred to the Web version of this article.)

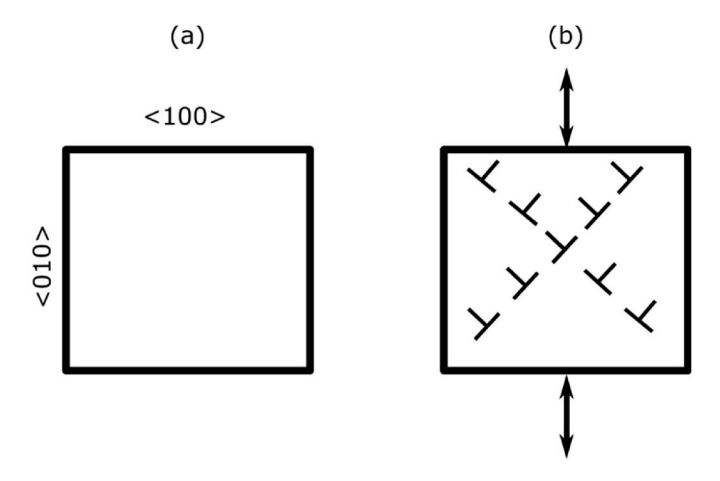


Fig. 2. Schematic diagram of the bulk model: (a) shows the crystal orientation at rest and (b) shows the bulk model under cyclic load and resulting dislocation pile-up.

concluded that softening is only possible due to the solute H interactions. In BCC Fe, no measurable effect was found on plastic flow [23]. However, this contradicts the in-situ experiment under microscope where an enhanced mobility due to H presence is widely observed [24]. Enhanced dislocation mobility should lead to softening, but no direct evidence of softening has been observed. At the microscale, Discrete Dislocation Dynamics (DDD) simulations shows that H increased dislocation velocity and crack propagation and decreased stacking fault energy [12]. The dislocation mobility law derived from DDD and H dependent core force derived from atomistic study inform the Crystal Plasticity models that investigate H effect on the texture evolution at the meso-scale [25]. Cohesive Zone Modeling (CZM) is another modeling tools used to study H embrittlement at the meso-scale by utilizing

traction-separation law where H reduces the cohesive energy at the cohesive zone [26]. At the continuum scale, phase field modeling techniques is used to model the effect of HELP by reducing yield stress as a function of H concentration [27].

Atomistic modeling is an effective tool to investigate a variety of phenomena where atomistic description of the material has a significant effect [27–33]. Since H embrittlement of metals occurs at an atomistic scale, atomistic modeling with a variety atomistic structure, interatomic potential and loading condition has been performed to understand specific aspects of H embrittlement mechanism. Through molecular dynamic simulation, Matsumoto et al. investigated H effect on the mode I crack propagation and estimated H trap energy in the vicinity of an edge dislocation [34]. Wang et al. showed that H inhibit <111>{112} slip promoting brittle fracture in the adjacent crack front. They also reported that H in {100} plane promotes martensitic transformation [35]. Li et al. emphasized on the H interaction with the grain boundary and demonstrated that H segregates into the grain boundary and hiders <100> grain boundary motion [36]. In a later study, they investigated the H embrittlement mechanism around $\Sigma 3$ grain boundary and reported that for Symmetric Incoherent Twin Boundary (SITB) H reduces the yield stress but for Inclined Twin Boundary H increases the yield stress [37]. Using Machine Learning based force field Zhang et al. studied crack propagation along pre-cracked sample for different grain boundaries [38]. Song et al. investigated the effect H on an edge dislocation mobility and pile-ups to understand the underlying nanoscale mechanism of HELP and reported H inhibiting dislocation mobility which the explained in terms of solute drag theory [39].

Local plastic deformation in metals is governed by dislocation nucleation, growth, existing dislocation density and dislocation mobility. Orowan's local kinematics law for metallic system relates these attributes as follows,

$$\dot{\lambda} = \rho v \overline{b} \tag{1}$$

where, local strain-rate $\dot{\lambda}$ depends on the local dislocation velocity ν and dislocation density ρ , \overline{b} being the Burgers vector which is constant for specific metallic systems. To truly understand how H impacts local plastic deformation (the HELP theory), it is vital to investigate its effect on both dislocation velocity and dislocation density.

This research aims to delve deeper into H's effect on these parameters through two series of atomistic modeling studies. The first examines how varying H concentrations influence an edge dislocation core velocity in single crystal iron under shear loads. Although screw dislocations are the primary carriers of dislocation in BCC iron, effect of H on the screw dislocation core has been found to be minimal compared to edge dislocation core due to the isotropic strain field induced by interstitial H [23,39–42]. The second investigates how increasing H concentrations affect dislocation accumulation. The following sections outline our Methodology, Results and Discussions, and finally, Conclusions are drawn from the two sets of results in the context of HELP mechanism.

2. Methodology

2.1. Atomistic modeling and simulation of H effect on dislocation mobility

Periodic Array of Dislocation (PAD) [43] model is used to model edge dislocation inside of a Single Crystal BCC Fe model. Periodic boundary condition (PBC) was used in the boundary along <111> and $<-1\cdot12>$ direction and shrink-wrapped boundary condition is used along the <-110> direction to be used as a traction boundary. A convergence analysis with energy minimization is performed to find the minimum dimensions of the PAD model with no significant periodic effect. As a result, the dimension for the PAD model was determined to be $61[111] \times 40[-110] \times 12[-1\cdot12]$ with 9480 atoms in pure Fe model. An edge dislocation with 1/2[111] Burgers vector is introduced at the

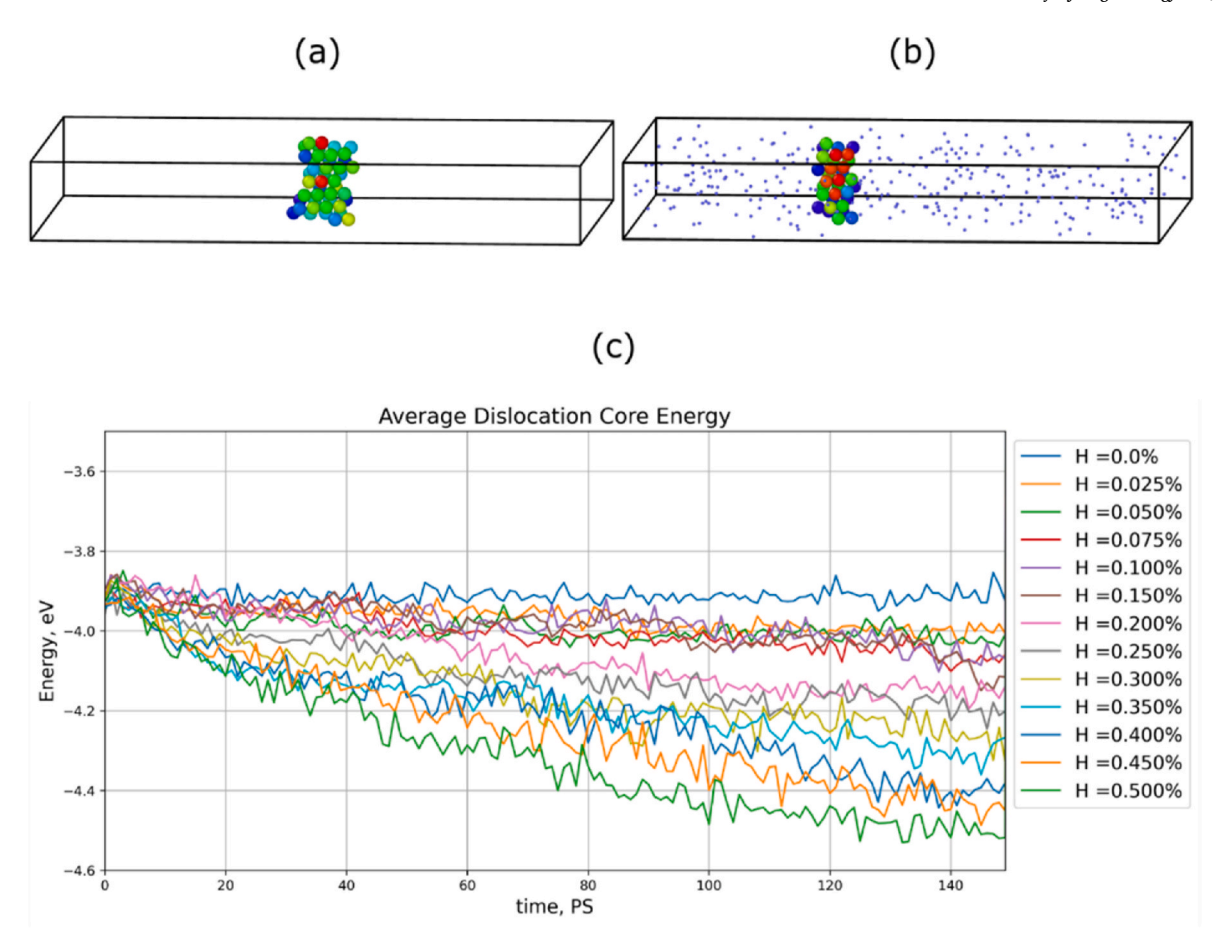


Fig. 3. H effect on dislocation core: (a) and (b) show the relative energy distribution in the edge dislocation core with and without H atoms, respectively. The average dislocation core energy with increasing H concentration is shown in (c).

 $\begin{tabular}{ll} \textbf{Table 1} \\ \textbf{Effect of H concentration on mobility of the Fe edge dislocation. Here, s and m denote sessile and mobile dislocation, respectively.} \\ \end{tabular}$

at% H	50 MPa	100 MPa	300 MPa	600 MPa	900 MPa	1200 MPa	1500 MPa
0.00	m	m	m	m	m	m	m
0.25	S	S	S	S	m	m	m
0.50	S	S	S	S	m	m	m
0.75	S	S	S	S	m	m	m
1.00	s	S	S	S	S	m	m

center of the $\{110\}$ plane by adding the upper half plane above the dislocation line by using the Atomsk software tool [44]. The schematic diagram of this PAD model with the edge dislocation is shown in Fig. 1a.

The widely used Large-Scale Atomic/Molecular Massively Parallel Software (LAMMPS) software is then used to perform a series of molecular dynamic (MD) simulations [45], as the bulk models are shown in the schematic diagram in Fig. 2. In the PAD model, at the traction boundary along [-110] direction, atoms that are 6 atomistic layers deep from the upper and lower region were marked to be frozen from thermal activation. For pure metal Fe, Embedded-Atom Method (EAM) potential developed by Proville et al. is used, which is particularly suitable for simulating glide of dislocations [46]. The PAD model is then equilibrated at 300 K temperature for 10 ps (ps), which was found to be sufficient to relax the pure Fe model. Care is taken not to include the frozen atoms in the equilibration process.

After the equilibrated configuration is obtained, a shear stress is applied on upper traction boundary along [-110]. A representative example of dynamic evolution of dislocation atomic structure and

dislocation velocity under shear is provided in the Supplemental Material. The total shear force is equally distributed among the upper frozen atoms as per the following equation,

$$force = \frac{stress}{lx * lz * n_{atoms}} \tag{2}$$

Where, lx and lz are the respective dimensions of the model along [111] and [-1-12], n_{atoms} is the number of atoms at the upper portion of the frozen atoms. The calculated per atoms forces are applied to the upper portion of the frozen atoms at each time step during the shear simulation. Shear stress varies from 0.1 GPa to 1.5 GPa for the PAD model keeping the temperature fixed at 300 K and shear simulation time at 150 ps. Due to the close vicinity of the core atoms to the frozen atoms where the shear force is applied, the applied shear stress gives a good estimation of the effective local shear stress at the dislocation core.

Open Visualization Tool (Ovito) is used to analyze the time-series data from molecular dynamic simulation [47]. To identify the local crystal structure, Ovito has two different tools based on distinct algorithms namely, Common Neighbor Analysis (CNA) [48] and Polyhedral Template Matching (PTM) [49]. CNA is a robust and efficient method that computes a fingerprint for pairs of atoms. However, CNA is more reliable for defect free atomistic structure with relaxed configuration. In the presence of strong thermal fluctuations and strain, the PTM method is determined to be a more reliable tool for structural identification. With the help of PTM, the atoms with native BCC crystal structure can be distinguished from dislocation core atoms with unmatched crystal structure as can be seen from Fig. 1c. The atoms that make up the dislocation core are marked and the average position of the collection of dislocation core atoms is recorded at each time step. This average

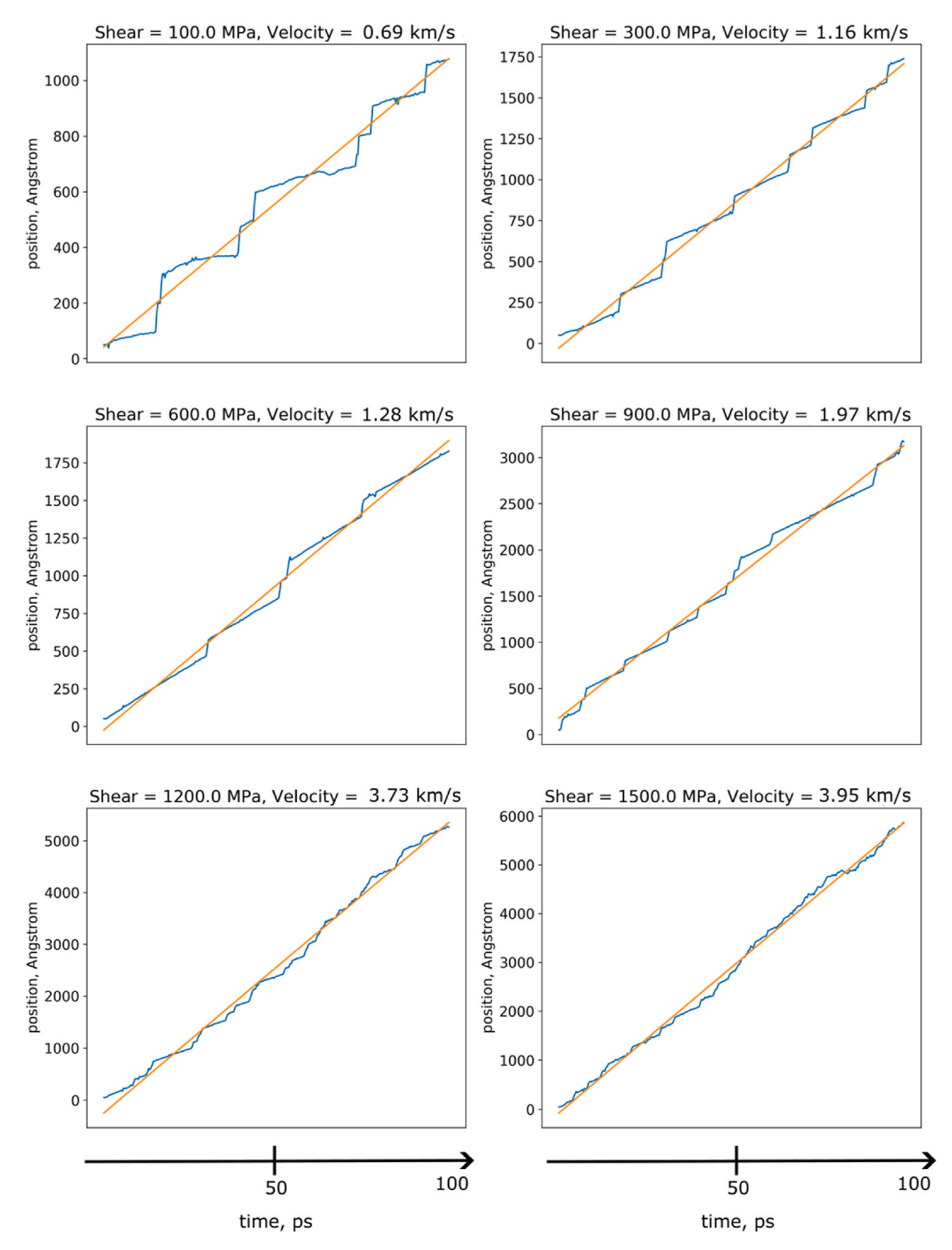


Fig. 4. Dislocation velocity with varying applied shear stress in pure Fe.

position of dislocation core atoms is plotted against time to calculate the edge dislocation velocity in pure Fe. To investigate the H effect on edge dislocation velocity, the PAD model is randomly incorporated with varying number of H atoms. After creating models with varying concentration of H (up to 1.0 at%), the simulation process of equilibration, shear and dislocation velocity calculation is performed on each model. Even though maximum H concentration in the charged sample is

reported around 0.1 at%, the local H concentration can rise by an order of magnitude, particularly at the defect sites like dislocation core [50].

2.2. Atomistic modeling and simulation of H effect on dislocation density

A bulk model of single crystal BCC Fe with dimension 20 nm \times 20 nm \times 40 nm is created. The pure Fe bulk model is comprised of

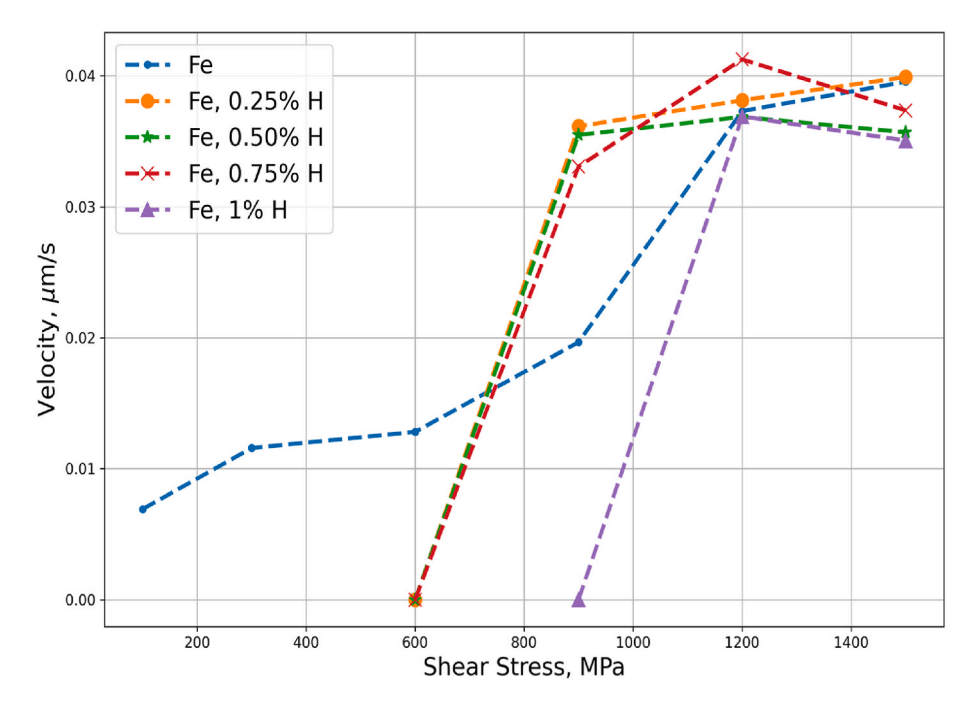


Fig. 5. Effect of H concentration on dislocation velocity in Fe.

1,372,000 Fe atoms. PBC conditions are applied along all directions to emulate the condition inside of Fe crystallite. The model was equilibrated at 300 K for 50 ps. After relaxed configuration is obtained, a fatigue load is applied on the relaxed model by introducing a periodic strain along the [010] direction. A representative example of dynamic evolution of dislocation accumulation under cyclic load is provided in the Supplemental Material. The periodic strain can be represented by the following equation,

$$y = ASin\left(\frac{2\pi n\delta T}{T_p}\right) \tag{3}$$

where, A denotes the magnitude of applied periodic deformation, n denotes the number of steps, δT denotes the timestep and T_p denotes the time period. This periodic strain or fatigue load is applied to the bulk model for 100 ps keeping the temperature at 300 K.

Dislocation Extraction Algorithm (DXA) is applied to the timeseries data of the MD simulation result [51]. Through this method, line representation of the individual dislocation is identified for different types of dislocations, and the length of these dislocations are also measured. The same MD simulation procedures are then repeated for models with 0.25 at%, 0.5 at%, 0.75 at% and 1.0 at% H and subsequent dislocation density is quantified.

3. Results and Discussions

3.1. H effect on dislocation mobility

The effect of H on the edge dislocation core at zero temperature is previously reported by Wang et al. where Peierls stress, shear modulus and dislocation core energy are computed at various H concentration [52]. Edge dislocation core energy is reported to show a steady decrease with the increase of H concentration from 0 to 0.08 at%. In the present work the effect of edge dislocation core configuration is computed at room temperature (300 K). Furthermore, to model H effect on Fe, the EAM potential developed by Wen [53] is used here as opposed to the Mendelev [54] potential as the former captures the repulsive effect of H–H interactions below 0.45 Å which is appropriate for modeling the behavior of H rich dislocation core.

Again, in the atomistic model, dislocation core atoms are identified

using the PTM method. The dislocation core energy then can be computed as the model is allowed to be equilibrated for 100 ps. Dislocation core atoms are at a higher energy compared to the rest due to the lattice mismatch. Fig. 3a and b shows that addition of H affects the energy distribution of the core and Fig. 3c shows that H atoms also affect the average energy of the core atoms. During equilibration, the average dislocation core energy of pure Fe remains constant but for the models with H atoms, dislocation core energy progressively reduces. This result shows the H atoms stabilize the dislocation core of Fe and the rate of stabilization directly correlates to the H concentration. Atomistic visualization reveals that the H atoms occupies the dislocation core interstitial position, reducing the lattice mismatch at the edge dislocation core which explains the reduction in core energy. The continuous reduction in core energy also confirms the progressive accumulation of H atom at the dislocation core.

The effect of this H induced stabilization of dislocation core on the mobility of dislocation is studied by analyzing the MD simulation result of application of shear load on the equilibrated models. The applied shear stress in the simulation is varied from 50 MPa to 1500 MPa whereas the H concentration varied from 0.25 % to 1.00 %. Table 1 shows the shear stress and H concentration at which the edge dislocation was able to mobilize. In pure Fe, the dislocation observed to be able to move at 50 MPa shear stress. However, with as little as 0.25 % presence of H, the dislocation is rendered immobile below 900 MPa shear stress. At 1.00 % H concentration, edge dislocation can only move at and above 1200 MPa applied shear.

At the applied shear and H concentration where dislocation can move, dislocation velocity is calculated from the slope of average dislocation core position against time curve. Fig. 4 shows how dislocation velocity changes with the increasing applied shear in pure Fe model. It can be noted that at lower applied shear stress, the dislocation core movement is non-linear, but as the applied shear increases, core movement becomes nearly linear. At low applied shear, atomistic lattices resist the core movement which then becomes insignificant with the increase of applied shear. This observation justifies the linear approximation to calculate dislocation velocity.

Even a small concentration of H dramatically modifies the dislocation core behavior as is observed from Table 1. Fig. 5 shows the effect of H concentration on dislocation velocity. While increase of H

2000

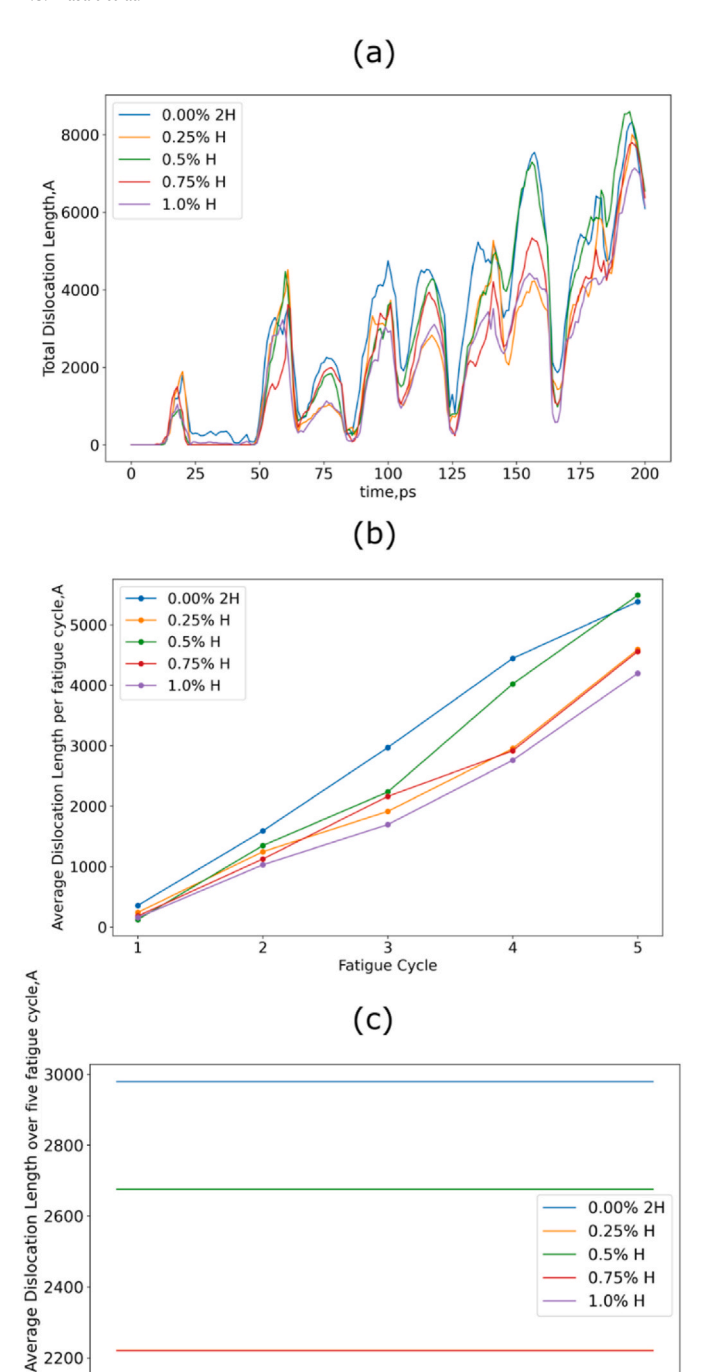


Fig. 6. Evolution of dislocation accumulation: (a), (b) and (c) show total dislocation length, cyclic average dislocation length and average dislocation length at varying H concentration, respectively.

100

time,ps

75

125

150

175

200

concentration increases the shear stress level required to mobilize an edge dislocation core, it also eases the initial lattice resistance when the level of shear stress is relatively low, enhancing the dislocation velocity compared to dislocation core in pure Fe. However, since at higher shear stress level (>900 MPa) lattice resistance does not play a significant part, this enhancement also becomes insignificant. Above 900 MPa shear stress, increasing H concentration starts to impede dislocation velocity. This can be explained by the fact that under high shear and larger dislocation velocity, lattice resistance is already small and thus, H

atoms only add to the viscus or phonon drag [55] on dislocation movement. Our modeling results on the H effect on dislocation mobility and other behaviors are in reasonable agreement with the reported experimental findings especially those obtained from electron microscopic studies [56–60].

3.2. H effect on dislocation nucleation and accumulation

Cyclic loading on the Fe bulk model with various H concentrations is simulated through MD simulation and DXA algorithm is used to study how H atoms affect dislocation accumulation. The motivation behind using cyclic loading as opposed to monotonic loading is to investigate the long-term dislocation accumulation in the model. During tension cycles, primarily dislocation nucleation occurs whereas during the subsequent compression cycle dislocation annihilation primarily takes place and thus, the accumulated dislocation is studied. In each simulation, the bulk model is subjected to tension for 20 ps and compression for 20 ps. A total of 5 tension-compression cycles are applied to quantify the dislocation accumulation pattern.

Fig. 6a shows the evolution of dislocation under the cyclic loading. Each peak dislocation count after the first cycle is associated with tension or compression state. It is observed that the peak dislocation length becomes progressively higher after each cycle. The inclusion of H initially (from 0.00 at%.to 0.75 at%) enhances maximum number of dislocations, resulting in higher peaks. However, at around 0.75–1.00 at % H concentration, the peak height of dislocation length decreased. Fig. 6b and c show the average accumulation of dislocation length over each cycle and 5 cycles (200 ps), respectively. It is observed that H concentration has a negative correlation with dislocation accumulation where with increasing H, dislocation accumulation gets suppressed.

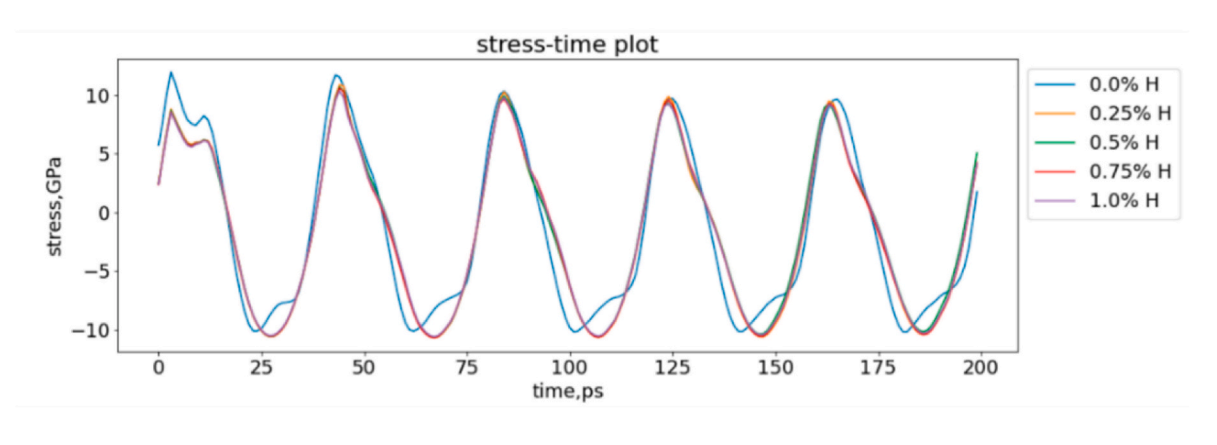
The above observation can be explained by the fact that H atoms occupies the interstitial position of the BCC lattice, increasing its rigidity and suppressing dislocation nucleation. Dislocation nucleation is the critical mechanism under the cyclic loading as dislocation nucleation and annihilation occurs during subsequent tension and compression cycle, respectively. As a result, newly nucleated dislocation makes up bulk of the dislocation line. This is different to monotonic loading where dislocation propagation and multiplication contribute to most existing dislocation. At lower H concentration, there are enough H-sparse regions where dislocation can be nucleated. The lattice misfit at the H-rich region acts as a significant obstacle that localizes the added stress during tension and compression. This led to enhancement in dislocation nucleation during tension and compression. As the H concentration is increased to around 0.75-1.00 at%, not enough H-sparse dislocation nucleation region remains which leads to suppression of the dislocation nucleation. The reduction of dislocation accumulation with increasing H concentration is explained by the suppression of dislocation nucleation at the H-rich region. It should be noted that the Kirchheim's defactant [61] theory which is rooted in the thermodynamic framework of solute-defect interactions posits that the inclusion of an external defactant like hydrogen increases the energy of the H charged free matrix consequently reducing the formation energy of the dislocation. While Kirchheim's theory represents a homogenized perspective, the atomistic suppression of dislocation nucleation revealed in the present study pertains to localized atomistic interactions.

Fig. 7a and b shows stress in response to the cycling loading. Addition of H significantly affects the stress response particularly in compression. The cyclic stress-strain curve shows that the stress-strain path shrinks over time signifying expected loss of strain energy to nucleate new dislocation. The addition of H further reduces the strain energy over time as it imposes an additional energy barrier to nucleate dislocation.

4. Conclusions

In conclusion, this study employs two separate sets of atomistic

(a)



(b)

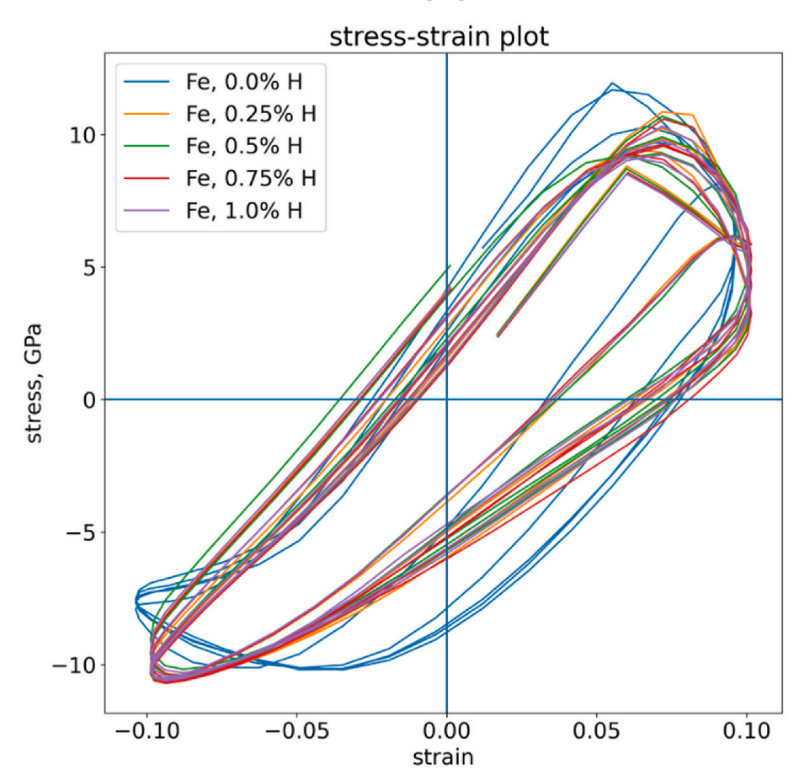


Fig. 7. Effect of H on stress response: (a) shows H effect on time evolution of stress response whereas (b) shows H effect on stress-strain relation.

simulations to probe the complex effects of hydrogen on dislocation mobility and density in iron. Key findings reveal a multifaceted influence of hydrogen atoms. First, they stabilize the edge dislocation core, thereby increasing the shear stress necessary for dislocation mobilization. Second, their impact on dislocation mobility is velocity-dependent: hydrogen facilitates mobility at low velocities by reducing lattice resistance but hampers it at high velocities due to increased viscus drag. Finally, dislocation nucleation varies with hydrogen concentrations, being suppressed in hydrogen-rich regions while amplified in areas with lower hydrogen levels. These nuanced insights offer a comprehensive understanding of how hydrogen interacts with dislocations, setting the stage for further research in this critical area.

Data availability

The raw/processed data required to reproduce these findings cannot

be shared at this time as the data also forms part of an ongoing study.

Declaration of competing interest

The authors declare that they have no known competing financial interests or personal relationships that could have appeared to influence the work reported in this paper.

Acknowledgements

This work was performed under the support of the US Department of Energy, Office of Basic Energy Sciences (Award No. SC0022244). S. Hasan wishes to thank the support of the US National Science Foundation, Division of Materials Research (Award No. 1900876). The authors wish to thank the High-Performance Computing Cluster (HPCC) at SDSU for providing computing support for this project. B. Bal acknowledges

the financial support by the Scientific and Technological Research Council of Turkey (TUBITAK) 3501 Career Development Program under Project No. 122M754.

Appendix A. Supplementary data

Supplementary data to this article can be found online at https://doi.org/10.1016/j.jjhydene.2023.12.274.

References

- [1] Xu WW, Tzanakis I, Srirangam P, Terzi S, Mirihanage WU, Eskin DG, Mathiesen RH, Horsfield AP, Lee PD. In situ synchrotron radiography of ultrasound cavitation in a molten Al-10Cu alloy. In: TMS2015 suppl. Proc.; 2015. p. 61–6. https://doi.org/10.1002/9781119093466.ch9.
- [2] Xu WW, Song XY, Li ED, Wei J, Zhang JX. Thermodynamic study on phase stability in nanocrystalline Sm-Co alloy system. J Appl Phys 2009;105. https://doi.org/ 10.1063/1.3129502.
- [3] Lu K. The Future of metals. Science 2010;328:319–20. https://doi.org/10.1126/ science.1185866.
- [4] Pradhan A, Vishwakarma M, Dwivedi SK. A review: the impact of hydrogen embrittlement on the fatigue strength of high strength steel. Mater Today Proc 2020;26:3015–9. https://doi.org/10.1016/j.matpr.2020.02.627.
- [5] Bal B, Koyama M, Gerstein G, Maier HJ, Tsuzaki K. Effect of strain rate on hydrogen embrittlement susceptibility of twinning-induced plasticity steel pre-charged with high-pressure hydrogen gas. Int J Hydrogen Energy 2016;41:15362–72. https:// doi.org/10.1016/j.ijhydene.2016.06.259.
- [6] Bal B, Sahin I, Uzun A, Canadinc D. A new venue toward predicting the role of hydrogen embrittlement on metallic materials. Metall. Mater. Trans. A Phys. Metall. Mater. Sci. 2016;47:5409–22. https://doi.org/10.1007/s11661-016-3708-7
- [7] Koyama M, Akiyama E, Lee YK, Raabe D, Tsuzaki K. Overview of hydrogen embrittlement in high-Mn steels. Int J Hydrogen Energy 2017;42:12706–23. https://doi.org/10.1016/j.ijhydene.2017.02.214.
- [8] Peter Cotterill. The hydrogen embrittlement of metals. Prog Mater Sci 1961;9: 205–301.
- [9] Barrera O, Bombac D, Chen Y, Daff TD, Galindo-Nava E, Gong P, Haley D, Horton R, Katzarov I, Kermode JR, Liverani C, Stopher M, Sweeney F. Understanding and mitigating hydrogen embrittlement of steels: a review of experimental, modelling and design progress from atomistic to continuum. J Mater Sci 2018;53:6251–90. https://doi.org/10.1007/s10853-017-1978-5.
- [10] Nagumo M, Takai K. The predominant role of strain-induced vacancies in hydrogen embrittlement of steels: overview. Acta Mater 2019;165:722–33. https://doi.org/ 10.1016/j.actamat.2018.12.013.
- [11] Sanchez J, Ridruejo A, de Andres PL. Diffusion and trapping of hydrogen in carbon steel at different temperatures. Theor Appl Fract Mech 2020;110:102803. https://doi.org/10.1016/j.tafmec.2020.102803.
- [12] Robertson IM, Sofronis P, Nagao A, Martin ML, Wang S, Gross DW, Nygren KE. Hydrogen embrittlement understood. Metall. Mater. Trans. A Phys. Metall. Mater. Sci. 2015;46:2323–41. https://doi.org/10.1007/s11661-015-2836-1.
- [13] Dadfarnia M, Nagao A, Wang S, Martin ML, Somerday BP, Sofronis P. Recent advances on hydrogen embrittlement of structural materials. Int J Fract 2015;196: 223–43. https://doi.org/10.1007/s10704-015-0068-4.
- [14] Li X, Yin J, Zhang J, Wang Y, Song X, Zhang Y, Ren X. Hydrogen embrittlement and failure mechanisms of multi-principal element alloys: a review. J Mater Sci Technol 2022;122:20–32. https://doi.org/10.1016/j.jmst.2022.01.008.
- [15] Zhou XW, El Gabaly F, Stavila V, Allendorf MD. Molecular dynamics simulations of hydrogen diffusion in aluminum. J Phys Chem C 2016;120:7500–9. https://doi. org/10.1021/acs.jpcc.6b01802.
- [16] Song J, Curtin WA. Atomic mechanism and prediction of hydrogen embrittlement in iron. Nat Mater 2012;12:145–51. https://doi.org/10.1038/nmat3479.
- [17] Tarleton E. Incorporating hydrogen in mesoscale models. Comput Mater Sci 2019; 163:282–9. https://doi.org/10.1016/j.commatsci.2019.03.020.
- [18] Kim S-G, Shin S-H, Hwang B. Machine learning approach for prediction of hydrogen environment embrittlement in austenitic steels. J Mater Res Technol 2022;19:2794–8. https://doi.org/10.1016/j.jmrt.2022.06.046.
- [19] He Y, Li Y, Chen C, Yu H. Diffusion coefficient of hydrogen interstitial atom in A-Fe, Γ-Fe and ε-Fe crystals by first-principle calculations. Int J Hydrogen Energy 2017;42:27438–45. https://doi.org/10.1016/j.ijhydene.2017.08.212.
- [20] Zhu S, Zhang C, Yang Z, Wang C. Hydrogen's influence on reduced activation ferritic/martensitic steels' elastic properties: density functional theory combined with experiment. Nucl Eng Technol 2017;49:1748–51. https://doi.org/10.1016/j. net.2017.08.021.
- [21] Teus SM, Shivanyuk VN, Shanina BD, Gavriljuk VG. Effect of hydrogen on electronic structure of fee iron in relation to hydrogen embrittlement of austenitic steels. Phys. Status Solidi Appl. Mater. Sci. 2007;204:4249–58. https://doi.org/ 10.1002/pssa.200723249.
- [22] Tehranchi A, Yin B, Curtin WA. Softening and hardening of yield stress by hydrogen-solute interactions. Philos Mag 2017;97:400–18. https://doi.org/ 10.1080/14786435.2016.1263402.
- [23] Tehranchi A, Curtin WA. The role of atomistic simulations in probing hydrogen effects on plasticity and embrittlement in metals. Eng Fract Mech 2019;216: 106502. https://doi.org/10.1016/j.engfracmech.2019.106502.

- [24] Birnbaum HK, Sofronis P. Hydrogen-enhanced localized plasticity-a mechanism for hydrogen-related fracture. Mater Sci Eng 1994;176:191–202. https://doi.org/ 10.1016/0921-5093(94)90975-X.
- [25] Messner MC, Rhee M, Arsenlis A, Barton NR. A crystal plasticity model for slip in hexagonal close packed metals based on discrete dislocation simulations. Model Simulat Mater Sci Eng 2017;25:44001. https://doi.org/10.1088/1361-651x/ 206872
- [26] Wu W, Wang Y, Tao P, Li X, Gong J. Cohesive zone modeling of hydrogen-induced delayed intergranular fracture in high strength steels. Results Phys 2018;11:591–8. https://doi.org/10.1016/j.rinp.2018.10.001.
- [27] Huang C, Gao X. Phase field modeling of hydrogen embrittlement. Int J Hydrogen Energy 2020;45:20053–68. https://doi.org/10.1016/j.ijhydene.2020.05.015.
- [28] Xu W, Maksymenko A, Hasan S, Meléndez JJ, Olevsky E. Effect of external electric field on diffusivity and flash sintering of 8YSZ: a molecular dynamics study. Acta Mater 2021;206:116596. https://doi.org/10.1016/j.actamat.2020.116596.
- [29] Xu W, Ramirez K, Gomez S, Lee R, Hasan S. A bimodal microstructure for fatigue resistant metals by molecular dynamics simulations. Comput Mater Sci 2019;160: 352–9. https://doi.org/10.1016/j.commatsci.2019.01.026.
- [30] Hasan MS, Lee R, Xu W. Deformation nanomechanics and dislocation quantification at the atomic scale in nanocrystalline magnesium. J Magnesium Alloys 2020;8:1296–303. https://doi.org/10.1016/j.jma.2020.08.014.
- [31] Hasan MS, Berkeley G, Polifrone K, Xu W. An atomistic study of deformation mechanisms in metal matrix nanocomposite materials. Mater Today Commun 2022;33:104658. https://doi.org/10.1016/j.mtcomm.2022.104658.
- [32] Xu W, Horsfield AP, Wearing D, Lee PD. Classical and quantum calculations of the temperature dependence of the free energy of argon. Comput Mater Sci 2018;144: 36–41. https://doi.org/10.1016/j.commatsci.2017.12.001.
- [33] Kapci MF, Schön JC, Bal B. The role of hydrogen in the edge dislocation mobility and grain boundary-dislocation interaction in α-Fe. Int J Hydrogen Energy 2021; 46:32695–709. https://doi.org/10.1016/j.ijhydene.2021.07.061.
- [34] Matsumoto R, Taketomi S, Matsumoto S, Miyazaki N. Atomistic simulations of hydrogen embrittlement. Int J Hydrogen Energy 2009;34:9576–84. https://doi. org/10.1016/j.ijhydene.2009.09.052.
- [35] Wang Z, Shi X, Yang X-S, He W, Shi S-Q, Ma X. Atomistic simulation of the effect of the dissolution and adsorption of hydrogen atoms on the fracture of α-Fe single crystal under tensile load. Int J Hydrogen Energy 2021;46:1347–61. https://doi. org/10.1016/j.jihydene.2020.09.216.
- [36] Li J, Lu C, Pei L, Zhang C, Wang R, Tieu K. Effects of H segregation on shear-coupled motion of (110) grain boundaries in α-fe. Int J Hydrogen Energy 2019;44: 18616–27. https://doi.org/10.1016/j.ijhydene.2019.05.071.
- [37] Li J, Pei L, Lu C, Godbole A, Michal G. Hydrogen effects on the mechanical behaviour and deformation mechanisms of inclined twin boundaries. Int J Hydrogen Energy 2021;46:16127–40. https://doi.org/10.1016/j. iihydene.2021.02.020.
- [38] Zhang B, Asta M, Wang LW. Machine learning force field for Fe-H system and investigation on role of hydrogen on the crack propagation in α-Fe. Comput Mater Sci 2022;214:111709. https://doi.org/10.1016/j.commatsci.2022.111709.
- [39] Song J, Curtin WA. Mechanisms of hydrogen-enhanced localized plasticity: an atomistic study using α-Fe as a model system. Acta Mater 2014;68:61–9. https:// doi.org/10.1016/j.actamat.2014.01.008.
- [40] Hirth JP. Effects of hydrogen on the properties of iron and steel. Metall Trans A 1980;11:861–90. https://doi.org/10.1007/bf02654700.
- [41] Birnbaum HK, Sofronis P. Hydrogen-enhanced localized plasticity{\textemdash}a mechanism for hydrogen-related fracture. Mater Sci Eng 1994;176:191–202. https://doi.org/10.1016/0921-5093(94)90975-x.
- [42] Wang S, Takahashi K, Hashimoto N, Isobe S, Ohnuki S. Strain field of interstitial hydrogen atom in body-centered cubic iron and its effect on hydrogen-dislocation interaction. Scripta Mater 2013;68:249–52. https://doi.org/10.1016/j. scriptamat.2012.10.026.
- [43] Bacon DJ, Osetsky YN, Rodney D. Chapter 88 dislocation-obstacle interactions at the atomic level. In: Dislocations in solids. Elsevier; 2009. p. 1–90. https://doi.org/ 10.1016/S1572-4859(09)01501-0.
- [44] Hirel P. Atomsk: a tool for manipulating and converting atomic data files. Comput Phys Commun 2015;197:212–9. https://doi.org/10.1016/j.cpc.2015.07.012.
 [45] Thompson AP, Aktulga HM, Berger R, Bolintineanu DS, Brown WM, Crozier PS, in
- [45] Thompson AP, Aktulga HM, Berger R, Bolintineanu DS, Brown WM, Crozier PS, in 't Veld PJ, Kohlmeyer A, Moore SG, Nguyen TD, Shan R, Stevens MJ, Tranchida J, Trott C, Plimpton SJ. LAMMPS a flexible simulation tool for particle-based materials modeling at the atomic, meso, and continuum scales. Comput Phys Comput. 2022;221:108171. https://doi.org/10.1016/j.cpc.2021.108171
- Commun 2022;271:108171. https://doi.org/10.1016/j.cpc.2021.108171. [46] Proville L, Rodney D, Marinica M-C. Quantum effect on thermally activated glide of dislocations. Nat Mater 2012;11:845–9. https://doi.org/10.1038/nmat3401.
- [47] Stukowski A. Visualization and analysis of atomistic simulation data with OVITO the Open Visualization Tool. Model Simulat Mater Sci Eng 2010;18:015012. https://doi.org/10.1088/0965-0393/18/1/015012.
- [48] Honeycutt JD, Andersen HC. Molecular dynamics study of melting and freezing of small Lennard-Jones clusters. J Phys Chem 1987;91:4950–63. https://doi.org/ 10.1021/j100303a014.
- [49] Larsen PM, Schmidt Sø, SchiØtz J. Robust structural identification via polyhedral template matching. Model Simulat Mater Sci Eng 2016;24:18. https://doi.org/ 10.1088/0965-0393/24/5/055007.
- [50] Zheng Z, Liang S, Zhu Y, Huang M, Li Z. Studying hydrogen effect on the core structure and mobility of dislocation in nickel by atomistically-informed generalized Peierls-Nabarro model. Mech Mater 2020;140:103221. https://doi. org/10.1016/j.mechmat.2019.103221.

- [51] Stukowski A, Albe K. Extracting dislocations and non-dislocation crystal defects from atomistic simulation data. Model Simulat Mater Sci Eng 2010;18:085001. https://doi.org/10.1088/0965-0393/18/8/085001.
- [52] Wang S, Hashimoto N, Ohnuki S. Hydrogen-induced change in core structures of {110}[111] edge and {110}[111] screw dislocations in iron. Sci Rep 2013;3. https://doi.org/10.1038/srep02760.
- [53] Wen M. A new interatomic potential describing Fe-H and H-H interactions in bcc iron. Comput Mater Sci 2021;197:110640. https://doi.org/10.1016/j.commatsci.2021.110640.
- [54] Mendelev MI, Han S, Srolovitz DJ, Ackland GJ, Sun DY, Asta M. Development of new interatomic potentials appropriate for crystalline and liquid iron. Philos Mag 2003;83:3977–94. https://doi.org/10.1080/14786430310001613264.
- [55] Queyreau S, Marian J, Gilbert MR, Wirth BD. Edge dislocation mobilities in bcc Fe obtained by molecular dynamics. Phys Rev B Condens Matter 2011;84. https://doi. org/10.1103/PhysRevB.84.064106.
- [56] Okada K, Shibata A, Gong W, Tsuji N. Effect of hydrogen on evolution of deformation microstructure in low-carbon steel with ferrite microstructure. Acta Mater 2022;225:117549. https://doi.org/10.1016/j.actamat.2021.117549.

- [57] Hwang C. The fundamentals of dislocation transport of hydrogen in bcc iron. Carnegit-Mellon University; 1984.
- [58] Gong P, Katzarov IH, Nutter J, Paxton AT, Rainforth WM. The influence of hydrogen on plasticity in pure iron—theory and experiment. Sci Rep 2020;10: 1–14. https://doi.org/10.1038/s41598-020-66965-z.
- [59] Huang L, Chen D, Xie D, Li S, Zhang Y, Zhu T, Raabe D, Ma E, Li J, Shan Z. Quantitative tests revealing hydrogen-enhanced dislocation motion in α -iron. Nat Mater 2023;22:710–6. https://doi.org/10.1038/s41563-023-01537-w.
- [60] Koyama M, Taheri-Mousavi SM, Taheri-Mousavi SM, Yan H, Kim J, Cameron BC, Moeini-Ardakani SS, Li J, Li J, Tasan CC. Origin of micrometer-scale dislocation motion during hydrogen desorption. Sci Adv 2020;6. https://doi.org/10.1126/ sciady.aar1187
- [61] Kirchheim R. Solid solution softening and hardening by mobile solute atoms with special focus on hydrogen. Scripta Mater 2012;67:767–70. https://doi.org/ 10.1016/j.scriptamat.2012.07.022.